# Supplemental Tables

| 3R Tau (263-280) numbering derived from 2N3R tau | | | | |
|---|---|---|---|---|
| **Name** | **Acetylation sites** | **K acetylated peptides** | **Name** | **K to Q mutant peptides** |
| R1R3 | | TENLKHQPGGGKVQIVYK | | |
| R1R3_1$_{Ac}$ | K267 | TENLK(Ac)HQPGGGKVQIVYK | R1R3_1$_{Q}$ | TENLQHQPGGGKVQIVYK |
| R1R3_2$_{Ac}$ | K274 | TENLKHQPGGGK(Ac)VQIVYK | R1R3_2$_{Q}$ | TENLKHQPGGGQVQIVYK |
| R1R3_3$_{Ac}$ | K311 | TENLKHQPGGGKVQIVYK(Ac) | R1R3_3$_{Q}$ | TENLKHQPGGGKVQIVYQ |
| R1R3_12$_{Ac}$ | K267,K274 | TENLK(Ac)HQPGGGK(Ac)VQIVYK | R1R3_12$_{Q}$ | TENLQHQPGGGQVQIVYK |
| R1R3_13$_{Ac}$ | K267,K311 | TENLK(Ac)HQPGGGKVQIVYK(Ac) | R1R3_13$_{Q}$ | TENLQHQPGGGKVQIVYQ |
| R1R3_23$_{Ac}$ | K274,K311 | TENLKHQPGGGK(Ac)VQIVYK(Ac) | R1R3_23$_{Q}$ | TENLKHQPGGGQVQIVYQ |
| R1R3_123$_{Ac}$ | K267,K274,K311 | TENLK(Ac)HQPGGGK(Ac)VQIVYK(Ac) | R1R3_123$_{Q}$ | TENLQHQPGGGQVQIVYQ |

| 4R Tau (263-280) numbering derived from 2N4R tau | | | | |
|---|---|---|---|---|
| **Name** | **Acetylation sites** | **K acetylated peptides** | **Name** | **K to Q mutant peptides** |
| R1R2 | | TENLKHQPGGGKVQIINK | | |
| R1R2_1$_{Ac}$ | K267 | TENLK(Ac)HQPGGGKVQIINK | R1R2_1$_{Q}$ | TENLQHQPGGGKVQIINK |
| R1R2_2$_{Ac}$ | K274 | TENLKHQPGGGK(Ac)VQIINK | R1R2_2$_{Q}$ | TENLKHQPGGGQVQIINK |
| R1R2_3$_{Ac}$ | K280 | TENLKHQPGGGKVQIINK(Ac) | R1R2_3$_{Q}$ | TENLKHQPGGGKVQIINQ |
| R1R2_12$_{Ac}$ | K267,K274 | TENLK(Ac)HQPGGGK(Ac)VQIINK | R1R2_12$_{Q}$ | TENLQHQPGGGQVQIINK |
| R1R2_13$_{Ac}$ | K267,K280 | TENLK(Ac)HQPGGGKVQIINK(Ac) | R1R2_13$_{Q}$ | TENLQHQPGGGKVQIINQ |
| R1R2_23$_{Ac}$ | K274,K280 | TENLKHQPGGGK(Ac)VQIINK(Ac) | R1R2_23$_{Q}$ | TENLKHQPGGGQVQIINQ |
| R1R2_123$_{Ac}$ | K267,K274,K280 | TENLK(Ac)HQPGGGK(Ac)VQIINK(Ac) | R1R2_123$_{Q}$ | TENLQHQPGGGQVQIINQ |

| 4R Tau (294-311) numbering derived from 2N4R tau | | | | |
|---|---|---|---|---|
| **Name** | **Acetylation sites** | **K acetylated peptides** | **Name** | **K to Q mutant peptides** |
| R2R3 | | KDNIKHVPGGGSVQIVYK | | |
| R2R3_1$_{Ac}$ | K294 | K(Ac)DNIKHVPGGGSVQIVYK | R2R3_1$_{Q}$ | QDNIKHVPGGGSVQIVYK |

| | | | | |
|---|---|---|---|---|
| R2R3_2$_{Ac}$ | K298 | KDNIK(Ac)HVPGGGSVQIVYK | R2R3_2$_{Q}$ | KDNIQHVPGGGSVQIVYK |
| R2R3_3$_{Ac}$ | K311 | KDNIKHVPGGGSVQIVYK(Ac) | R2R3_3$_{Q}$ | KDNIKHVPGGGSVQIVYQ |
| R2R3_12$_{Ac}$ | K294, 298 | K(Ac)DNIK(Ac)HVPGGGSVQIVYK | R2R3_12$_{Q}$ | QDNIQHVPGGGSVQIVYK |
| R2R3_13$_{Ac}$ | K294, 311 | K(Ac)DNIKHVPGGGSVQIVYK(Ac) | R2R3_13$_{Q}$ | QDNIKHVPGGGSVQIVYQ |
| R2R3_23$_{Ac}$ | K298, 311 | KDNIK(Ac)HVPGGGSVQIVYK(Ac) | R2R3_23$_{Q}$ | KDNIQHVPGGGSVQIVYQ |
| R2R3_123$_{Ac}$ | K294,298,K311 | K(Ac)DNIK(Ac)HVPGGGSVQIVYK(Ac) | R2R3_123$_{Q}$ | QDNIQHVPGGGSVQIVYQ |

| **4R Tau (325-343) numbering derived from 2N4R tau** | | |
|---|---|---|
| **Name** | **Acetylation sites** | **K acetylated peptides** |
| R3R4 | | LGNIHHKPGGGQVEVKSEK |
| R3R4_1$_{Ac}$ | K331 | LGNIHHK(Ac)PGGGQVEVKSEK |
| R3R4_2$_{Ac}$ | K340 | LGNIHHKPGGGQVEVK(Ac)SEK |
| R3R4_3$_{Ac}$ | K343 | LGNIHHKPGGGQVEVKSEK(Ac) |
| R3R4_123$_{Ac}$ | K331, K340, K343 | LGNIHHK(Ac)PGGGQVEVK(Ac)SEK(Ac) |

| **4R Tau (357-374) numbering derived from 2N4R tau** | | |
|---|---|---|
| **Name** | **Acetylation sites** | **K acetylated peptides** |
| 4RR’ | | LDNITHVPGGGNKKIETH |
| 4RR’_1$_{Ac}$ | K369 | LDNITHVPGGGN(Ac)KIETH |
| 4RR’_2$_{Ac}$ | K370 | LDNITHVPGGGNK(Ac)IETH |
| 4RR’_12$_{Ac}$ | K369, K370 | LDNITHVPGGGNK(Ac)K(Ac)IETH |

**Table S1. Nomenclature and sequences for all peptides used in the study. Related to Figures 1 and 2.** The site of acetylation or glutamine mutation is indicated by “Ac” and “Q”, respectively, and is colored in red. All peptides were N-terminally acetylated and C-terminally amidated.

## Supplemental Figures and Legends

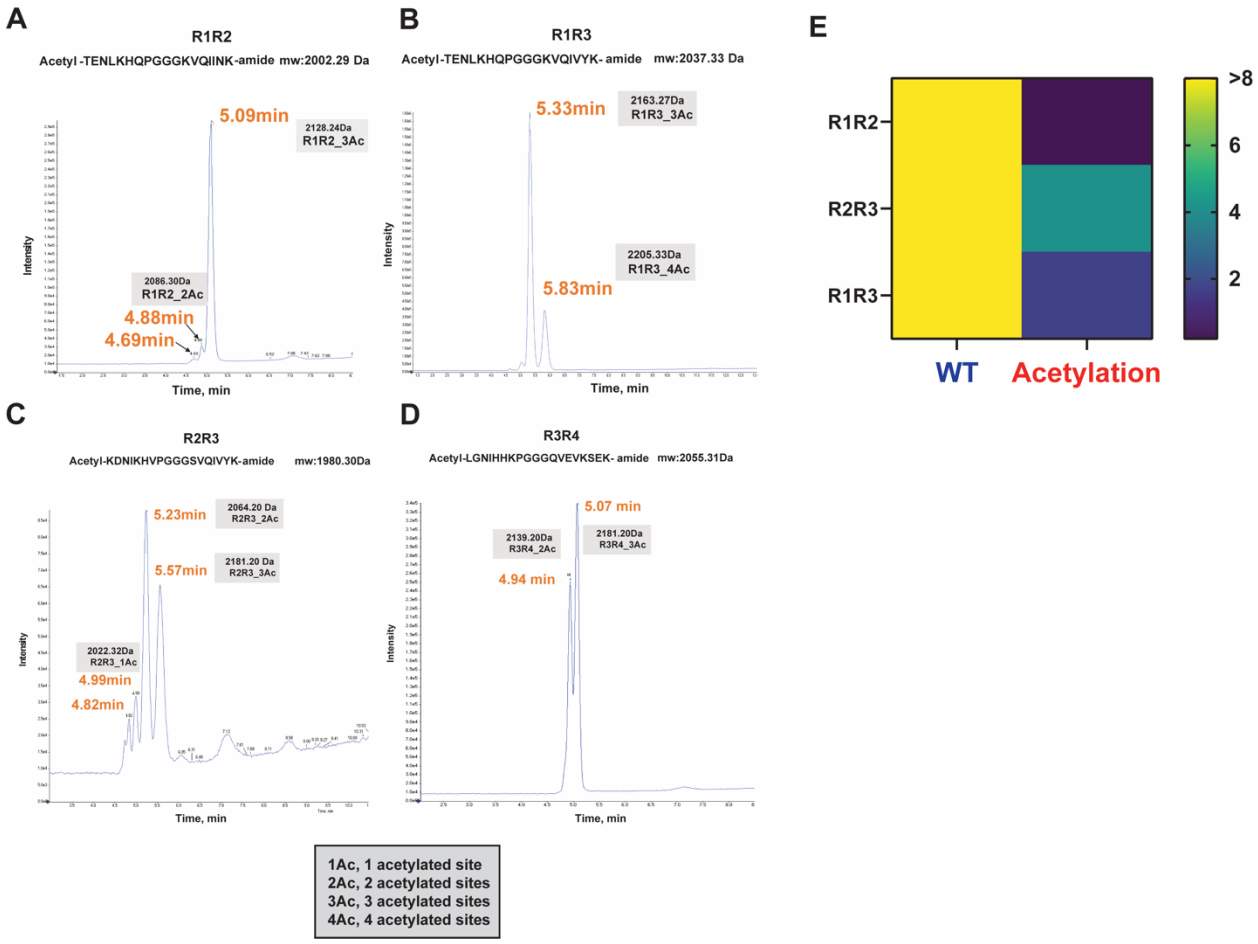


**Figure S1. Validation of chemical modification of the R1R2, R2R3, R3R4 and R1R3 peptides. Related to Figure 1.** Mass spectrometry analysis of chemically acetylated R1R2 (**A**), R1R3 (**B**), R2R3 (**C**) and R3R4 (**D**) peptides. The masses for each peptide species are indicated with annotation of how many lysines are modified. **E.** Estimation of $t_{1/2max}$ from the ThT fluorescence aggregation curves for chemically acetylated vs control peptides shown in Figure 1D. For peptides that remained flat over the 8 days experiment we estimate the $t_{1/2max} > 8$ (yellow). For peptides that aggregated within 8 days, the values are colored from blue to cyan. Aggregation experiments were performed in triplicate. The data were fit to a non-linear regression model fitting in GraphPad Prism to estimate an average $t_{1/2max}$.

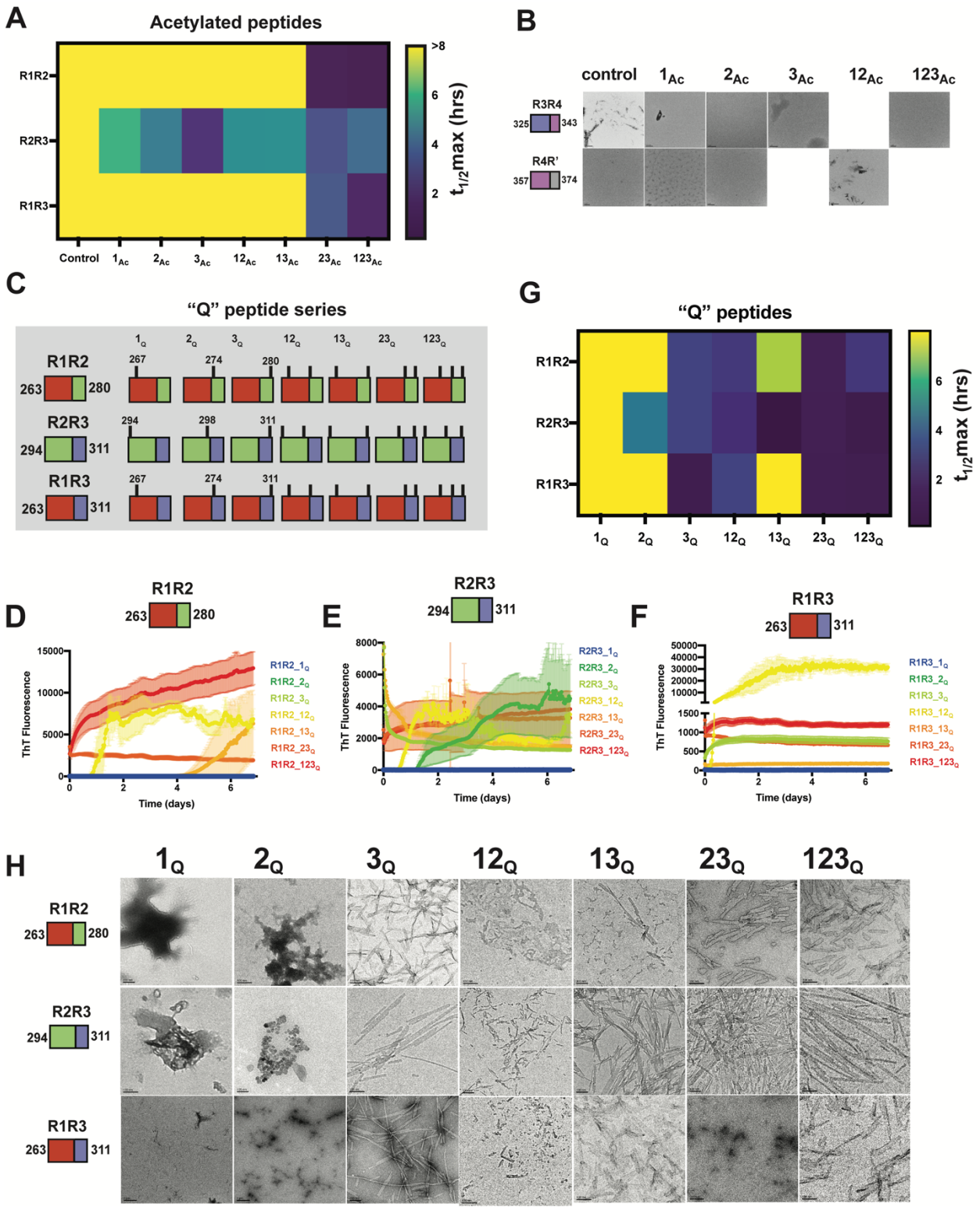


**Figure S2. Patterns of acetylation and glutamine mutation that drive model tau peptide aggregation. Related to Figure 2. A**. Estimation of $t_{1/2max}$ from the ThT fluorescence aggregation curves for unmodified, mono-, di- and tri-acetylated R1R2, R2R3, R3R4 and R1R3

peptides in Figure 2C-F. For peptides that remained flat over the 8 days experiment we estimate the $t_{1/2max} > 8$ (yellow). For peptides that aggregated within 8 days, the values are colored from blue to cyan. Aggregation experiments were performed in triplicate. The data were fit to a non-linear regression model fitting in GraphPad Prism to estimate an average $t_{1/2max}$. **B**. TEM images of ThT fluorescence aggregation assay end products from control (WT) and the R3R4 and R4R' acetylated peptides from aggregation experiments shown in Figure 2F. Scale bars indicate 0.5-1µm. **C**. Illustration of the tau peptide series with all combinatorial glutamine mutations at lysine sites for the R1R2, R2R3 and R1R3 tau peptides. Sequences are colored by repeat domain as in Figure 1A. Acetylation sites are indicated by ticks above the cartoon for each peptide. ThT fluorescence aggregation experiments of the R1R2 (**D**), R2R3 (**E**) and R1R3 (**F**) unmodified and glutamine mutated series. Curves are colored by the number of modifications from blue (control) to red (all lysines mutated to glutamine modified). Aggregation experiments were performed in triplicate and the averages are shown with standard deviation. The data were fit to a non-linear regression model fitting in GraphPad Prism to estimate an average $t_{1/2max}$ (**G**). **H**. TEM images of ThT fluorescence aggregation assay end products from control and glutamine substituted R1R2, R2R3 and R1R3 peptides from aggregation experiments shown in Figure S2D-F. Scale bars indicate 0.1 µm.

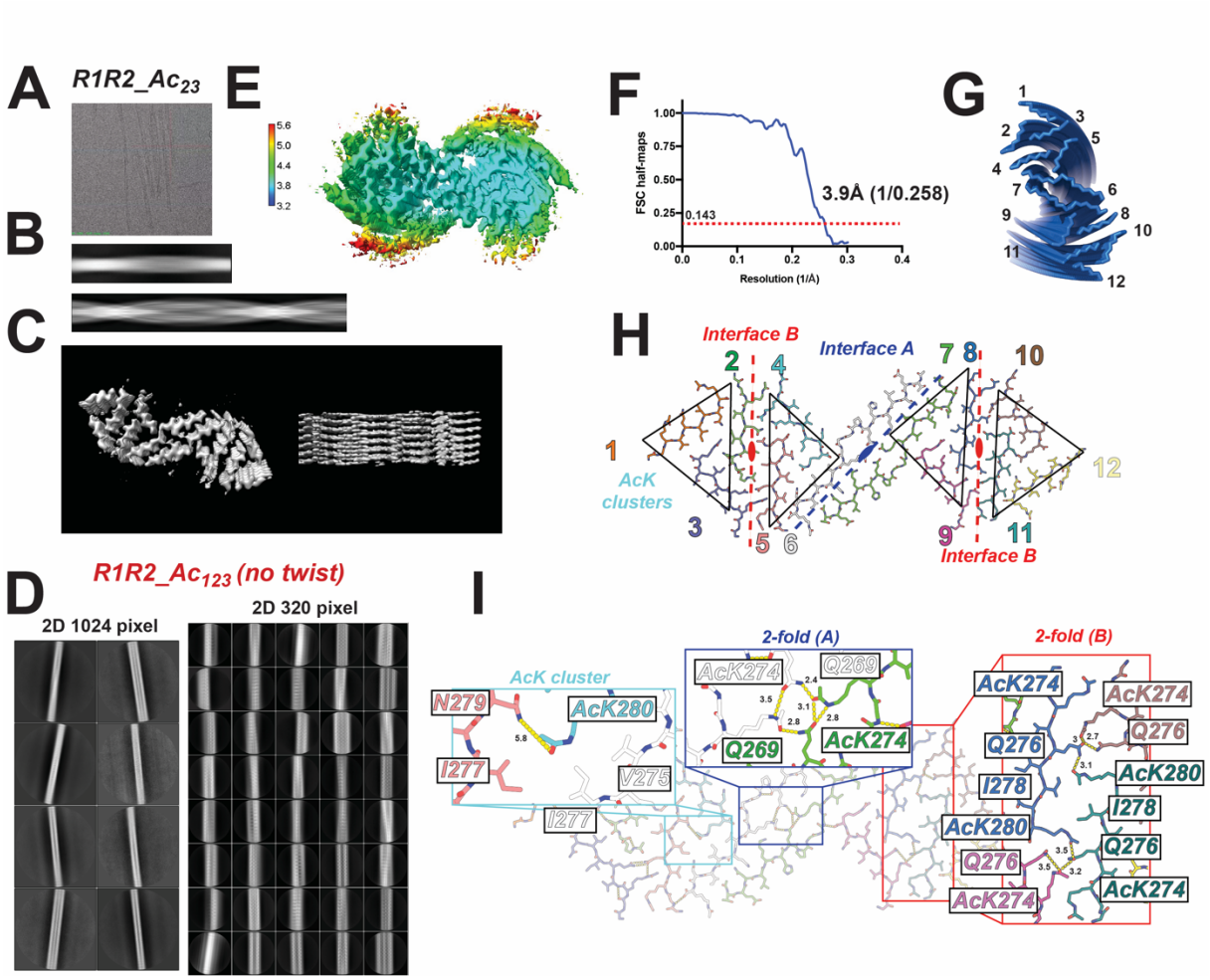


**Figure S3. Map quality and analysis of interfaces of the R1R2 $23_{Ac}$ fibril structure. Related to Figure 3. A.** View of the R1R2 $23_{Ac}$ fibril on a cryo-EM grid. **B**. 2D projection of the R1R2 $23_{Ac}$ fibril. **C.** 3D map of the R1R2 $23_{Ac}$ fibril contoured at 7 σ**. D.** 2D projection of the fully acetylated R1R2 fibril (i.e. R1R2 $123_{Ac}$) at 1024 and 320 pixels at 0.86Å/pixel revealing little twist. **E.** Local resolution map of the R1R2 $23_{Ac}$ assembly. The map is colored by resolution ranging from blue to red. **F.** Fourier Shell Correlation (FSC) curve for refined half-maps of R1R2 $23_{Ac}$. **G.** Illustration of the arrangement of the 12 fragments in a single layer. **H.** Visualization of the symmetric interactions observed within a layer of our fibril assembly comprised of 12 independent chains from 1 to 12. The central interface formed between two extended fragments is annotated as “Interface A” and is defined a 2-fold symmetry axis between monomers 6-7 (blue). “Interface B” is defined by a pseudo 2-fold symmetric interactions between K(Ac)VQIINK(Ac) and K(Ac)VQIINK(Ac) from monomers 2-5 and 8-11 (red). The “interface B” interaction is flanked by a triangular interaction centered on a lysine acetylation site, termed “AcK cluster” formed between monomers 1-2-3 and 10-11-12. Structure is shown as sticks with all-atom and colored by fragment. **I.** illustration of the interactions at the different symmetric interfaces. Interface A is stabilized by three hydrogen bonds formed between two acetylated lysines at 274 and two glutamine 276 within a layer. Interface B is stabilized by symmetric interactions between K(Ac)VQIINK(Ac): K(Ac)VQIINK(Ac) mediated between I278 and I278

nonpolar contacts as as well as hydrogen bonds between acetylated K274 and Q276 from two different chains. AcK cluster is stabilized by interactions between three fragments involving nonpolar contacts between I277, I277, V275 and acetylated K280. Structure is shown as sticks with backbone and side chains.

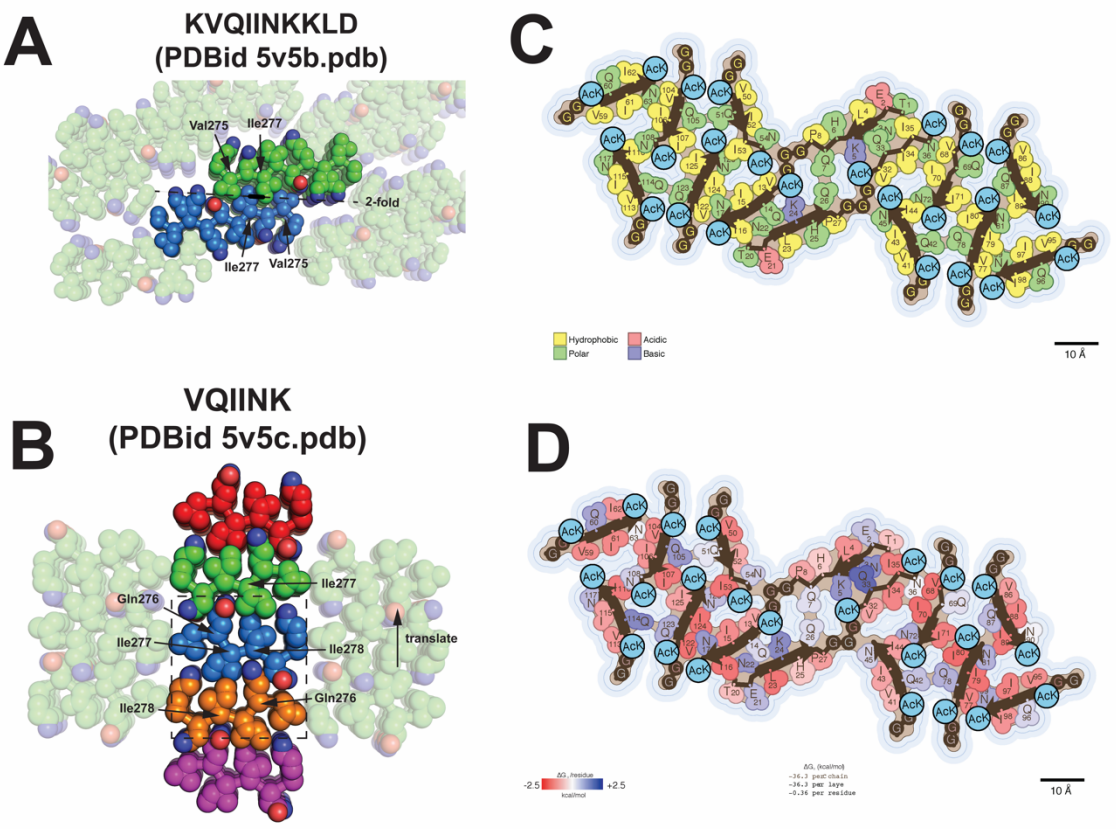


**Figure S4. Key stabilizing interactions in R1R2 23$_{Ac}$ fibril are consistent with structures of isolated amyloid motif fragments. Related to Figure 4. A.** 2-fold symmetric interactions observed in X-ray structures of KVQIINKKLD (PDB id 5v5b.pdb) stabilized by interactions between V275 and I277. Structures are shown in spheres (all-atom) representation and the key interactions are highlighted. The central dimer is highlighted and the peripheral interactions are shown with transparency. **B.** X-ray structures of VQIINK (PDB id 5v5c.pdb) reveal a screw axis core dimer interaction (dashed box) that is reproduced via translation in the lattice. This interaction is stabilized by contacts between I278 and I278 with interlayer Q279 hydrogen bonding. The core of the interactions are shown as spheres (all-atoms) and colored by chain. Peripheral interactions are shown with transparency. **C**. Single layer view of the R1R2 23Ac structure highlighting the amino acid property composition across the 12 fragments. Nonpolar, polar, acidic, basic, and acetyl-lysine are colored yellow, green, red, blue and baby blue, respectively. **D**. Solvation energy estimation of per residue contribution to the stability of the monolayer. Destabilizing residues are colored in blue (+2.5 kcal/mol) and stabilizing residues are colored red (-2.5 kcal/mol).

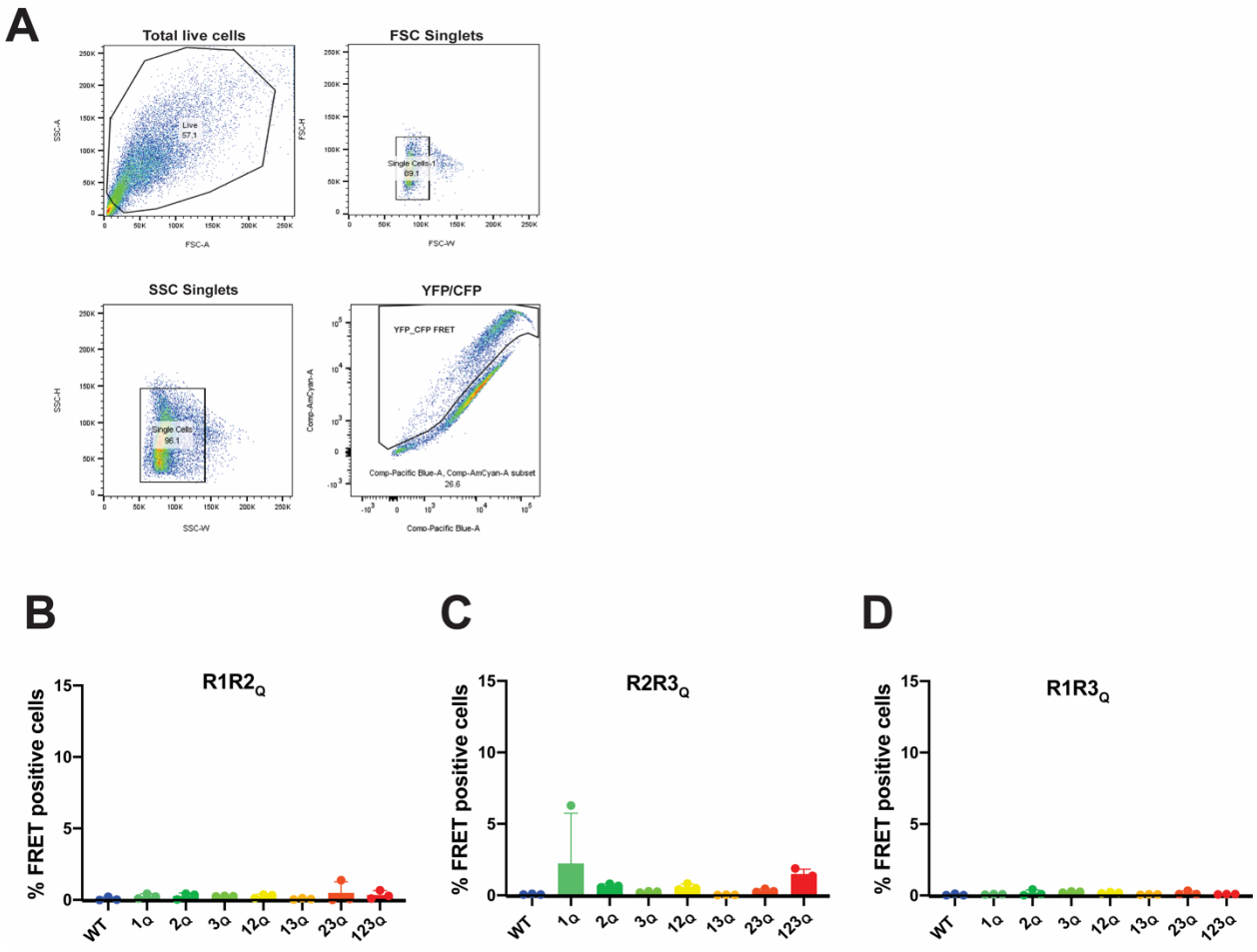


**Figure S5. Cell-based evaluation of seeding capacity of aggregated acetylated or glutamine substituted tau peptides. Related to Figure 5. A.** Flow cytometry strategy to quantify FRET between intracellular mClover3 and mCerulean tau aggregates. Quantification of FRET signal across control and glutamine substituted "Q" peptides transduced into the tau biosensor cells: R1R2 (**B**), R2R3 (**C**) and R1R3 (**D**). Bar plots are colored as in Figure S2. Data is shown as averages across three experiments with error bars representing a 95% CI of each condition.